International Journal of Chemical Science
www.chemicaljournals.com
Online ISSN: 2523-2843
Received: 10-05-2026, Accepted: 10-06-2026, Published: 25-06-2026
Volume 10, Issue 2, 2026, Page No. 95-105

Design, synthesis, and biological evaluation of novel 6-aminobenzothiazole -based zink (Ii) metal complexes with anticancer, antimicrobial, adme applications and dna-binding studies

K Jagadesh babu[1*], Koyada Vivek[2]
[1] Department of Chemistry, Government Degree College, Parkal, Hanamkonda, Telangana, India
[2] Department of Computer Science (AIML), S.R.M University Tiruchirappalli, Tamil Nadu, India
Corresponding Author: K Jagadesh babu
DOI: https://doi.org/10.66856/chemical.2026.10.2.10033

Abstract
Two novel Zn(II) complexes derived from 6-aminobenzothiazole-based Schiff base ligands (HL_1 and HL_2) were synthesized and comprehensively characterized using spectroscopic and analytical techniques, including mass spectrometry, FT-IR, UV–Vis spectroscopy, magnetic susceptibility, and thermogravimetric analysis (TGA). The complexes, formulated as $[Zn(HL)_2(H_2O)_2]$, were found to exhibit a six-coordinate octahedral geometry. DNA binding studies suggested an intercalative interaction mode for the complexes, with binding constants (K_a) following the order 2a > 1a, as determined by UV absorption and emission experiments. In DNA cleavage assays, the complexes demonstrated higher efficiency in cleaving double-stranded pBR322 DNA through oxidative and photolytic methods compared to their parent Schiff base. Cytotoxicity assays against A549 and MCF7 cell lines showed enhanced activity for the complexes relative to the free ligands. Additionally, *In-vitro* antimicrobial studies confirmed the superior efficacy of the complexes over the ligands. The biological efficacy of the ligands (HL_1 & HL_2) and their complexes (1a & 2a) was further validated through computational methods, including ADME analysis using the SWISS ADME tool. The in silico studies indicated that both the ligands and complexes exhibit drug-like properties and promising bioavailability, highlighting their potential as oral drugs.

Keywords: Metal complexes, DNA interaction, ADME, Anti bacterial, Antifungal, cytotoxic activity

Introduction

Coordination compounds are important in medicinal chemistry because transition metal ions can modulate the biological and physicochemical properties of molecules in ways that purely organic compounds cannot achieve efficiently [1, 2]. Among the various ligands used in coordination chemistry, Schiff bases are particularly attractive due to their facile synthesis, structural versatility, and strong coordination through nitrogen and oxygen donor atoms [3, 4]. Metal complexes of Schiff bases have been widely reported to exhibit antimicrobial, anticancer, antioxidant, and antiviral activities [5, 6]. Their anticancer potential is often associated with interactions with DNA, which can disrupt replication and transcription processes and induce apoptosis [7, 8]. Transition metal complexes have also shown promise in managing metabolic disorders such as diabetes through inhibition of carbohydrate-metabolizing enzymes and reduction of oxidative stress [9, 10]. Complexation with biologically relevant metal ions frequently enhances activity by increasing lipophilicity and improving cellular uptake [11–13]. In particular, zinc-based complexes have attracted attention because of their comparatively lower toxicity and favorable biological profile.

In this study, we report the synthesis and characterization of novel Zn(II) complexes derived from Schiff bases obtained from 6-aminobenzothiazole and halogen-substituted salicylaldehydes. The complexes were evaluated for their thermal stability, antibacterial activity, cytotoxic effects, and DNA-binding interactions to explore their potential as biologically active metal-based agents.

Material and Methods

1. Materials

All of the preparatory materials and solvents were procured from Sigma-Aldrich, Merck, and Hi Media Ltd. The solvents used for the synthesis were thoroughly distilled and dried according to standard methods. The Supercoiled pBR322 DNA and CT-DNA were purchased from Genei in Bangalore, India, and kept at 4 °C. Double-distributed water was used to prepare all of the buffer solutions for the DNA binding and cleavage experiments.

2. Methods

The elemental analysis (C, H, N and S) of all the synthesised compounds was performed using a Perkin-Elmer elemental analyzer. FT-IR spectra were recorded on the Perkin-Elmer Infrared Model 337 in the range 4000-250 cm^{-1}. UV-Vis spectra of compounds were analysed on a Shimadzu UV-Vis 2600 spectrophotometer in DMSO solvent in the range between 200 and 800 nm. ESI mass spectra were recorded on an HP-LC mass spectrometer (Agilent Tech, USA). The metal content of the complexes was determined using atomic absorption spectroscopy with the GBC Avanta 1.0 AAS. The melting points of the compounds were determined on a Polmon instrument (model No.MP-96. The thermo gravimetric analysis (TGA) of all metal complexes were carried out in a dynamic nitrogen atmosphere with a heating rate of 10 °C min^{-1} on a Shimadzu TGA-50H in the temperature range of 27–1200 °C. Fluorescence spectra were recorded on a Shimadzu RF-5301PC spectrofluorometer.

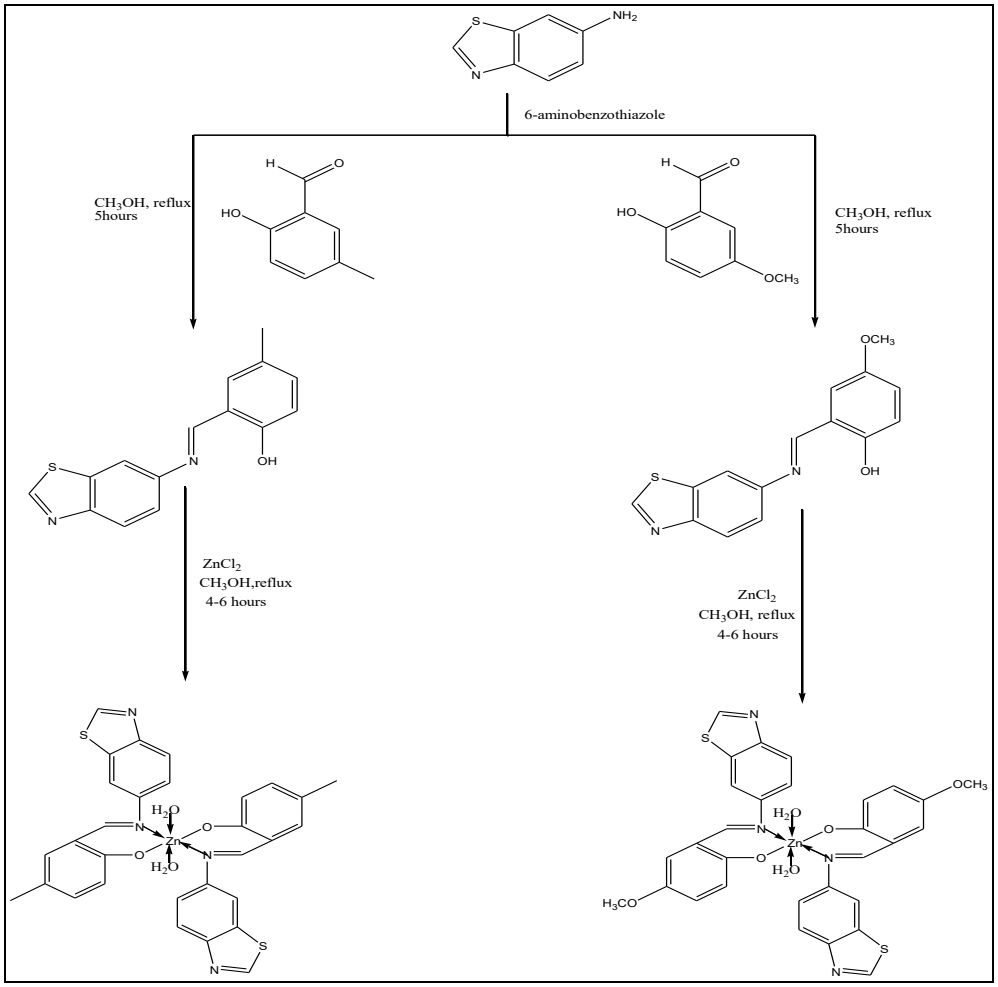

Scheme 1: Synthesis of Schiff base and corresponding 1a and 2a complexes

3. Synthesis of Schiff base Ligansds (HL_1 and HL_2)

The ligands HL_1 and HL_2 were synthesized according to a previously reported procedure [14, 15]. The synthetic route is illustrated in Scheme 1.

2-Benzo[*d*]thiazol-6-ylimino)methyl)-4-methylphenol ($C_{15}H_{12}N_2OS$)(HL_1)

Yield:79%. Elamental Analysis. Calcd (%): C, 67.14; H, 4.51; N, 10.44; S, 11.95. Found: C, 67.10; H, 4.43; N, 10.40; S, 11.88, Melting Point: 90-95 ºC. IR (KBr): $\nu_{(O-H)}$ 3428, $\nu_{(CH=N)}$ 1616, $\nu_{(C-O)}$ 1153, (Fig. S1). UV-Vis; lmax/nm (cm-1): 282 (35460), 313 (31948), 359 (27855), (Fig.S2). ^{1}H NMR (400 MHz, CDCl3) δ: **):** 12.85 (s, 1H); 8.98 (s, 1H); 8.65 (s, 1H); 8.15 (d, J = 8.7 Hz, 1H); 7.83 (d, J = 2.0 Hz, 1H); 7.46 (dd, J_1 = 2.25Hz, J_2 = 8.7 Hz, 1H); 7.22 (s, 1H); 7.20 (s, 1H); 6.95 (dd, J_1 = 2.7 Hz, J_2 = 6.2 Hz, 1H); 2.33 (s, 3H), (Fig. S3). 163.3, 158.9, 154.1, 152.1, 146.5, 134.9, 134.4, 132.4, 128.3, 124.1, 120.2, 118.7, 117.1, 114.1, 20.3, (Fig. S4). LC-MS (m/z): Calc: 268.7: Found: 269 $[M+H]^+$ [15].

2-Benzo[*d*]thiazol-6-ylimino)methyl)-4-methylphenol ($C_{15}H_{12}N_2O_2S$)(HL_2)

Yield: 75%; M.p: 101-105 °C; Anal. Calc (%):C, C, 63.36; H, 4.25; N, 9.85; S, 11.28. Found: C, 63.26; H, 4.18; N, 9.74; S, 11.22; IR (KBr): $\nu_{(O-H)}$ 3435, $\nu_{(CH=N)}$ 1623, $\nu_{(C-O)}$ 1164, (Fig. S1). UV-Vis: lmax/nm (cm-1); 265 (37735), 282 (35460), 315 (31746), 374 (26737), (Fig-S2). ^{1}H NMR (400 MHz, CDCl3): δ; 12.64 (s, 1H); 8.94 (s, 1H); 8.57 (s, 1H); 8.14 (d, J = 8.2 Hz, 1H); 7.75 (s, 1H); 7.41 (d, J = 8.5 Hz, 1H); 6.96 (s, 2H); 6.86 (s, 1H); 3.77 (s, 3H), (Fig. S3). ^{13}C NMR (100 MHz, CDCl3): δ; 162.8, 155.3, 154.2, 152.3, 152.1, 146.1, 134.9, 124.0, 120.7, 120.1, 118.7, 118.0, 115.3, 114.1, 55.8, (Fig. S4). ESI–MS (m/z):Calc: 285.8, Found: 285 $M+H]^+$ [14].

Synthesis of binary metal complexes (1a-2a)

The Zink metal complexes 1a and 2a were synthesized reacting the Schiff base ligands with the corresponding metal salts in a 1:2 (metal:ligand) molar ratio. A hot methanolic solution (10 mM) of $Zncl_2$ was added drop wise to a hot, magnetically stirred methanolic solution of the Schiff base ligands (HL_1/HL_2) (20 mM). The reaction mixture was refluxed at 70–80 °C for 4–6 h with continuous stirring, and the progress of complex formation was monitored periodically. Upon completion, the resulting colored solid complexes were isolated by filtration, washed successively with hot methanol and petroleum ether to remove unreacted materials and impurities, and then dried in a vacuum desiccator over anhydrous $CaCl_2$. The general synthetic route for the ligands and their corresponding metal complexes (1a and 2a) is illustrated in Scheme 1.

[$Zn(HL_1)_2(H_2O)_2$]: ($C_{30}H_{26}N_4O_4S_2Zn$) (1a)

Colour: light orange Yield: 78%, M.pt: ~105-108 ºC, Anal. Found. (Cal.) C, 56.21(56.65); H, 4.38 (4.12); Zn, 10.01 (10.28); N, 8.26 (8.81); S, 10.32 (10.08); IR (KBr) (cm-1): ν(O-H) 3438: ν(HC=N) 1602, ν(C–O) 1146, ν(M–O) 530, ν(M–N) 468; 810; 752 UV-Vis (DMSO) λmax/nm (cm-1): 258 (38759), 303 (33003), 426 (23474); μeff (BM): 0; MS (ESI): m/z 636 $[M+2]^+$ (Figure 3. 1a).

$[Zn(HL_2)_2(H_2O)_2]$: ($C_{30}H_{26}N_4O_4S_2Zn$) (2a)
Color: yellowish orange, Yield: 76%, M.pt: ~120-123 ºC, Anal. Found. (Cal.) C, 56.27(56.65); H, 4.46 (4.12); Zn, 10.11 (10.28); N, 8.65 (8.81);S, 10.01 (10.08); IR (KBr) (cm^{-1}): ν(O-H) 3467: ν(HC=N) 1606, ν(C–O) 1139, ν(M–O) 527, ν(M–N) 469; 829; 756; UV-Vis (DMSO) λmax/nm (cm^{-1}): 257 (38910), 329 (30395), 438 (22831); μeff (BM): 0; MS (ESI): m/z 668 $[M+2]^+$ (Figure 3. 2a).

4. DNA binding studies

UV–Vis spectroscopic studies

The DNA binding affinities of two monometallic complexes 1a and 1b were assessed using the UV-visible absorption method. The complex concentration maintained constant of 10μM, while the concentration of CT-DNA varied from 0 to 10 μM. The complexes were initially dissolved in DMSO due to limited solubility in buffer solution. To prepare the CT-DNA stock solution, DNA was diluted in a Tris-HCl/NaCl buffer at pH = 7.2 (50mM NaCl/5 mM Tris-HCl). The purity of the CT-DNA was ensured by measuring UV spectra using molar extinction coefficient of 6600 M^{-1} at 260 nm [14,15]. Mixing the CT-DNA solution with the respective complex and reference solution, followed by five minutes incubation before recording the absorption spectra. By analyzing the absorption data we determined the intrinsic binding constant (K_b) for interaction of each complex with CT-DNA.

Fluorescence quenching study

Using fluorescence spectrophotometer and EB-bound CT-DNA in Tris HCl/NaCl buffer (pH 7.2), the binding between metal complexes and CT-DNA was investigated. The emission spectra of CT-DNA (125 μM) bound to EB (12.5 μM) were captured in the 360–800 nm region (350 nm excitation) as complex quantities were varied from 0 to 60 μM. The comparative binding affinity of the complexes with CT-DNA was calculated using the quenching constant derived by the Stern-Volmer equation [15], Io/I = 1 + Ksv r. The fluorescence (emission band) intensities in the absence and presence of complexes are denoted by I_o and I, respectively; K_{sv} is a linear Stern-Volmer constant; and 'r' is the complex concentration as a proportion of the DNA concentration.

DNA cleavage

The ability of schiff base and its monometallic metal compounds (1a, 1b and 1c) to cleave DNA was evaluated using agarosegel electrophoresis in the presence and absence of H_2O_2. Super coiled pBR322 DNA was diluted in a Tris-HCl/NaCl buffer at pH 7.2, and treated with varying concentrations of the metal complexes [16]. After a two hour incubation at room temperature, bromophenol blue (2μL) was added to the DNA sample followed by vigorous stirring. The sample was then loaded onto a 1% agarosegel containing a TAE buffer (PH 8.0) and subjected to electrophoresis at 70 V for 45 minutes. Prior to electrophoreses, the gel was stained with ethidiumbromide. The resulting gel is photographed using the BIO-RAD Gel documentation system, and the DNA bands were observed under transilluminators.

5. Biological Evaluation

Antimcrobial activity

The *in vitro* antimicrobial activity of the synthesized Schiff base ligands (HL_1 and HL_2) and their corresponding metal complexes (1a and 2a) was evaluated using the agar well diffusion method. Antibacterial activity was assessed against two Gram-positive bacterial strains, Staphylococcus aureus and Bacillus subtilis, and two Gram-negative bacterial strains, Escherichia coli and Klebsiella pneumoniae. Gentamycin sulphate was used as the standard antibacterial drug. Freshly prepared bacterial cultures were grown for 24 h and uniformly spread onto sterile nutrient agar plates. Wells of 6 mm diameter were made in the agar medium using a sterile cork borer. The test compounds were introduced into the wells at concentrations of 25, 50, and 75 μg/well. The inoculated plates were incubated at 25 ± 2 °C, and the antibacterial activity was determined by measuring the diameter of the inhibition zones (mm) surrounding each well. The results were compared with those obtained for the standard drug.

Antifungal activity was evaluated against Aspergillus niger and Candida albicans using the same agar well diffusion technique. One-week-old fungal cultures were used as inocula, and Nystatin served as the reference antifungal agent. The antifungal efficacy of the compounds was determined by measuring the diameter of the inhibition zones (mm) and comparing the results with those of the standard drug.

Anticancer activity (MTT assay)

Synthesized substances (HL_1, HL_2, 1a, and 2a) were tested for their cytotoxicity on A-549 and MCF-7 cell lines. Cell viability was determined using the MTT assay. Tumour cells were cultured in 25 cm^2 flasks with appropriate medium at 37 °C in a CO_2 incubator. MCF-7 and A-549 cells were separately plated in a 96-well plate. After overnight growth, the cells were switched to low serum media. DMSO was used as the control. After 48 hours of exposure to different synthesized substances, the cells were treated with MTT solution for 4 hours. Then, the medium was removed. Optical density at 570 nm was measured using an ELISA plate reader, representing cell quantity. The results were reported as a percentage of cytotoxicity/viability. Every experiment was taken in triplicates, and the cytotoxicity of the test substance Doxorubicin was compared to determine the IC_{50} values.

ADME predictions

Online computational approaches have revolutionized the prediction of ADME properties of compounds. These methods offer a cost-effective and time-efficient alternative to *in vivo* experiments for predicting drug characteristics. Numerous in silico methods utilize molecular structure, pharmacokinetic, and physicochemical data to forecast ADME parameters. A comprehensive ADME prediction analysis was performed using the Swiss ADME tool (http://www.swissadme.ch) to assess the ADME properties of the Schiff base and its metal complexes [17].

Results and discussion

The Schiff base ligands and their corresponding metal complexes were successfully synthesized and characterized using spectral and elemental analyses. The synthesized Zn(II) complexes are colored, non-hygroscopic and stable at room temperature. They are soluble in DMF, DMSO, and acetonitrile, but insoluble in water. The obtained analytical data are in good agreement with the calculated values, confirming the proposed compositions. Furthermore, the results indicate that the metal-to-ligand stoichiometry in these complexes is 1:2.

1. FT-IR Spectroscopy

FT-IR spectroscopy is a valuable technique for identifying functional groups and elucidating the coordination behavior of ligands with metal ions, including chelation and denticity. The FT-IR spectra of the Schiff base ligands and their metal complexes were recorded at room temperature over the range of 4000–250 cm^{-1} using KBr pellets.

The Schiff base ligands HL_1 and HL_2 exhibited characteristic azomethine (C=N) stretching bands at 1616 and 1623 cm^{-1}. Upon complexation, these bands shift by approximately 14-17 cm^{-1}, indicating the participation of the azomethine nitrogen in coordination with the metal ion [18]. A broad band observed at 3428 cm^{-1} for HL_1 and 3435 cm^{-1} for HL_2, assigned to the phenolic –OH group, disappears after complexation, confirming the formation of a metal–oxygen (M-O) bond via the phenolic oxygen [19]. Moreover, the C-O stretching bands appear at 1153 cm^{-1} for HL_1 and 1164 cm^{-1} for HL_2. In the metal complexes, these bands shift to slightly lower frequencies by 7-25 cm^{-1}, further supporting coordination through the phenolic oxygen atom. New bands appearing in the regions 527-530 cm^{-1} and 468-469 cm^{-1} in the complexes are attributed to M-O and M-N stretching vibrations, respectively [20]. A broad band observed at 3438 and 3467 cm^{-1} in complexes 1a and 2a indicates the presence of coordinated water molecules within the coordination sphere [21]. Furthermore, an additional set of bands appeared in the range of 810–829 cm-1 and 752–756 cm^{-1}. These bands are attributed to the rocking and wagging vibrations, which further supports the existence of coordinated water molecules in the complexes.

These spectral features clearly demonstrate that the ligands coordinate to the metal ions in a bidentate manner through both azomethine nitrogen and phenolic oxygen atoms, as illustrated in Figures 1. 1a and 2a.

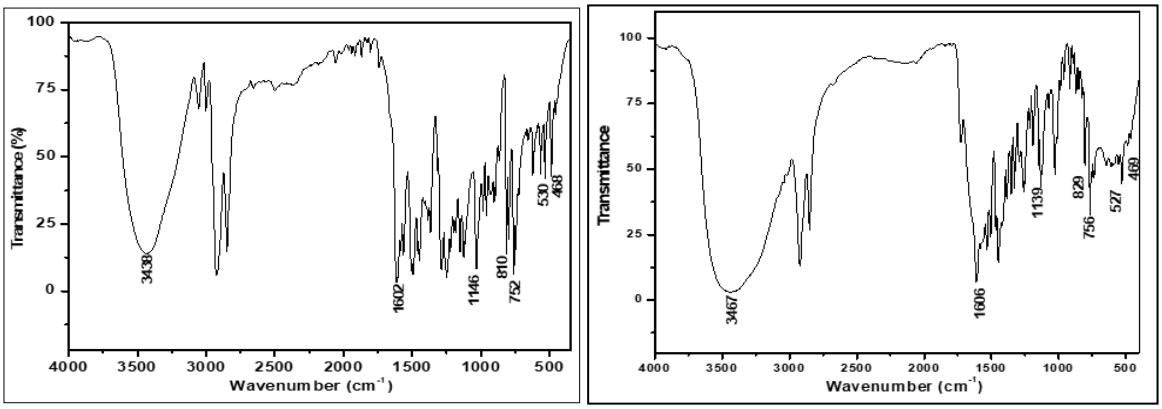

1a **2a**

Fig 1: FTIR spectrum of metal complexes 1a, and 2a in the region of 4000-250 cm^{-1}

Table: 1. IR frequencies (cm-1) of Schiff base ligand and its metal complexes.

COMPOUND	$\vartheta(O-H)$ cm^{-1}	$\vartheta(C=N)$ cm^{-1}	$\vartheta(C-O)$ cm^{-1}	$\vartheta(M-O)$ cm^{-1}	$\vartheta(M-N)$ cm^{-1}
HL_1	3428	1616	1153		
HL_2	3435	1623	1164		
1a	3438 (810, 752)	1602	1146	530	468
2a	3467 (829, 756)	1606	1139	527	469

2. ESI Mass Spectral Studies

ESI mass spectrometry provides useful information about the molecular structure of a compound. The mass spectra of the metal complexes 1a and 2a showed molecular ion peaks at m/z = 636 ($[M+2]^+$) for 1a and m/z = 668 ($[M+2]^+$) for 2a (Figures 3. 1a and 2a). These peaks confirm the formation of metal complexes with a $[M(L)_2]$ composition. The mass spectral results, along with elemental analysis, support a 1:2 metal-to-ligand ratio in the complexes.

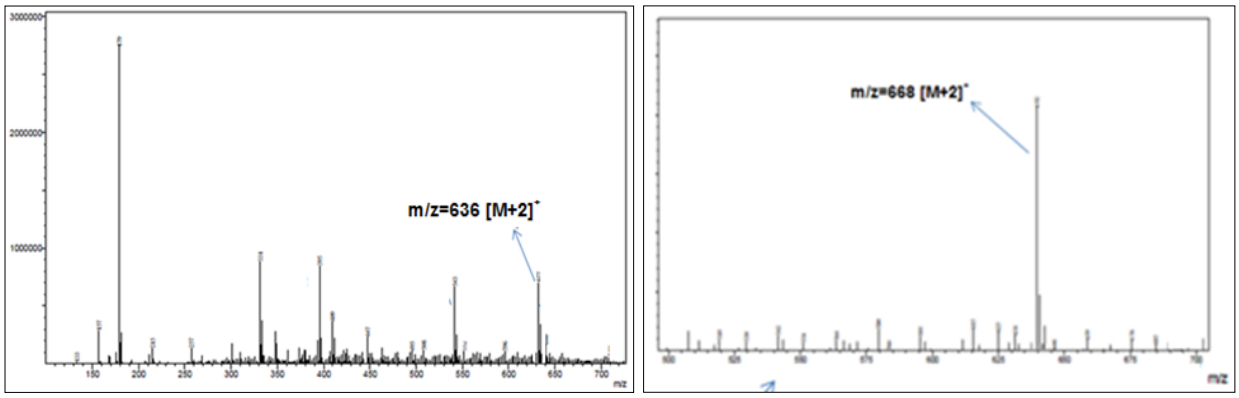

1a **2a**

Fig 3: ESI- Mass spectrum (positive ion mode) of the metal complexes 1a, and 2a

3. Electronic Spectra and Magnetic Moments

The electronic spectra of the synthesized Schiff base ligands HL_1 and HL_2 and their corresponding metal complexes (1a and 1b) were measured at room temperature using DMSO as the solvent. The spectral data are summarized in Table 2 and depicted in Figures 2.1a and S2.1b.

The free Schiff base ligands display two prominent absorption bands in the regions 265-282 nm (3773-3546 cm^{-1}) and 313- 374 nm (3194–2673 cm^{-1}), which are assigned to π→π transitions within the aromatic rings and n→π* transitions of the azomethine (C=N) group, respectively. In the metal complexes, these bands shifted to 257–258 nm (3891–3875 cm^{-1}) and 303–329 nm (3300 – 3039 cm^{-1}), indicating coordination between the ligand and the metal ions [22]. Furthermore, an additional absorption band emerges in the region 426–438 nm (2347–2283 cm^{-1}) in the metal complexes 1a and 1b respectively, which is absent in the free ligands.

This band is attributed to ligand-to-metal charge transfer (LMCT) transitions [23]. Owing to the d^{10} electronic configuration of Zn(II), d–d transitions are not observed in its complexes. The effective magnetic moments of complexes 1a and 2a are found to be zero, confirming their diamagnetic nature. Overall, these spectral characteristics support the successful coordination of the Schiff base ligands with the metal ions.

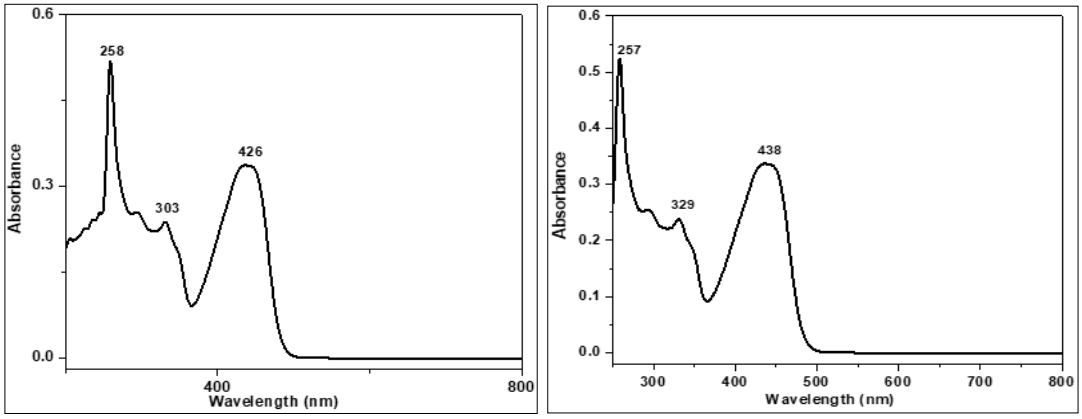

1a **2a**

Fig 4: UV-Vis spectra of spectrum of metal complexes 1a, and 2a in the region of 200-800nm

Table 2: magnetic momentum and electronic spectra of schiff base and its metal complexes 1a, and 2a

Compound	π -π*	n–π*	CT bands	μ_{effect}
HL_1	282 (35460 cm^{-1})	313 (31948 cm^{-1})		
HL_2	265 (37735), 282 (35460 cm^{-1})	315 (31746), 374 (26737 cm^{-1})		
1a	258 (38759 cm^{-1})	303 (33003 cm^{-1})	426 (23474 cm^{-1})	0
2a	257 (38910 cm^{-1})	329 (30395 cm^{-1})	438 (22831 cm^{-1})	0

4. Thermo gravimetric analysis

Thermogravimetric analysis (TGA) of complexes 1a and 2a revealed a three-stage decomposition pattern (Figure 4). Both complexes remain thermally stable up to 106–122 °C, indicating the absence of lattice solvent molecules. The first weight loss, observed between 129–136 °C, is attributed to the elimination of two coordinated water molecules. The second stage corresponds to ligand degradation, where complex 1a exhibits a sharp mass loss over the temperature range of 242–495 °C, while complex 2a shows a sudden weight loss between 285–320 °C, indicating partial decomposition of the organic ligand framework. In the final stage, complex 1a undergoes gradual degradation in the temperature range of 790–1050 °C, whereas complex 2a displays a rapid weight loss between 510–619 °C. This stage is associated with the complete decomposition of the organic moiety, ultimately leading to the formation of the corresponding metal oxide residue [22, 23].

Based on the combined interpretation of spectral studies and analytical data, the structures of the complexes are proposed as $[Zn(HL_1)_2(H_2O)_2]$ for complex 1a and $[Zn(HL_2)_2(H_2O)_2]$ for complex 2a (Scheme I).

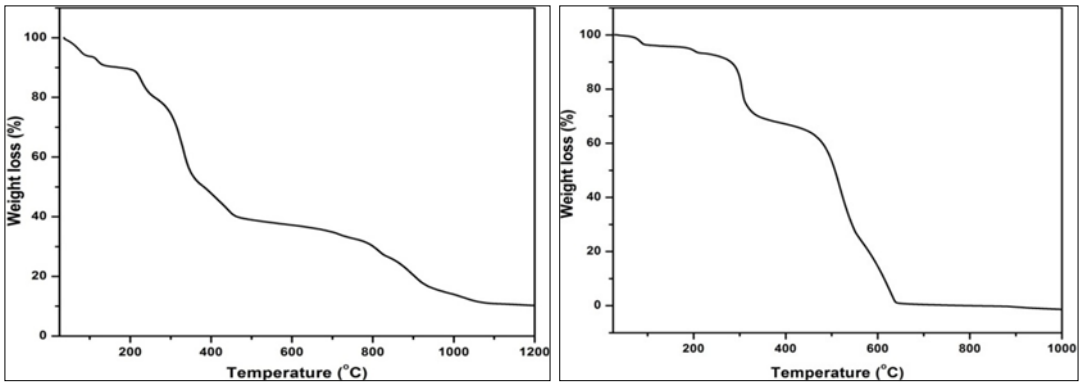

1a **2a**

Fig 5: TGA curve of complex 1a and 2a

5. DNA binding studies

Electronic absorption study

In the current study, the interactions between CT-DNA and the metal complexes 1a and 2a were examined, and the changes in absorbance with and without CT-DNA are shown in Figure 4. Complexes 1a and 2a displayed absorption bands in the range of 257-258 nm, attributed to intra-ligand π–π* transitions. Upon the addition of CT-DNA, a decrease in absorbance (hypochromism) along with a slight red shift (bathochromic shift) was observed, suggesting that the metal complexes interact with DNA through an intercalation mode [24]. To estimate the intrinsic binding constant (Kb) of the complexes with CT-DNA, the equation $[DNA]/(\varepsilon_a-\varepsilon_f) = [DNA]/(\varepsilon_b-\varepsilon_f)+1/K_b(\varepsilon_b-\varepsilon_f)$ was used. In this equation, [DNA] is the concentration of CT-DNA (in base pairs), Kb is the intrinsic binding constant, εa is the apparent molar absorptivity (A_{obsd}/[complex]), and εf and εb are the molar extinction coefficients of the free and bound forms of the complex, respectively. The calculated binding constants were $1.342 \pm 0.02 \times 10^5$ M^{-1} for complex 1a and $2.135 \pm 0.02 \times 10^5$ M^{-1} for complex 2a [25]. These findings confirm that both complexes have a strong binding affinity for CT-DNA, with complex 2a showing greater binding strength than complex 1a. (For comparison, ethidium bromide has a K_b of 7×10^7 M^{-1}).

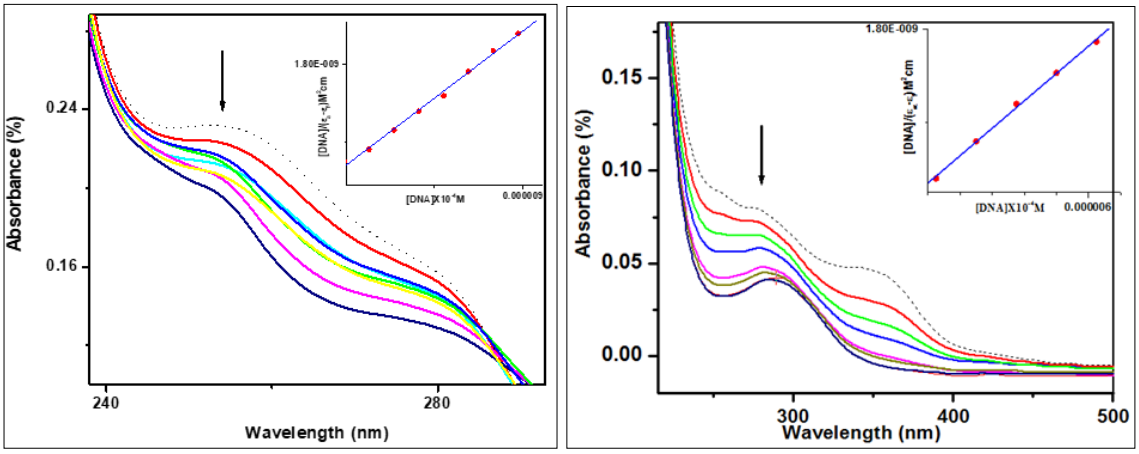

1a 2a

Fig 6: UV-Vis absorption spectra of complexes 1a and 2a in Tris-HCl buffer (pH 7.2) at 25 °C in the presence (solid line) and absence (dashed line) of an increase in concentration of CT-DNA. For the determination of the intrinsic binding constant, Kb, for DNA binding, see the inset linear plot

Fluorescence quenching study

Fluorescence analysis using the emission intensity of the probe ethidium bromide (EB) was used to study the binding strength of metal complexes 1a and 2a with CT-DNA. In Tris-HCl buffer, EB shows weak fluorescence. When EB binds to CT-DNA by inserting between DNA base pairs (intercalation), its fluorescence intensity increases significantly [26, 27]. However, adding metal complexes to the EB-DNA system reduces this fluorescence, suggesting that the complexes compete with EB for DNA binding through an intercalative mode [28], as shown in Figure 4. The strongest emission of EB-DNA is observed between 593–598 nm.

The Stern–Volmer quenching constants (Ksv), obtained from fluorescence quenching data, revealed that complex 2a has a higher binding affinity than 1a. The Ksv values were $9.6 \pm 0.02 \times 10^3$ M^{-1} for 1a and $1.4 \pm 0.02 \times 10^4$ M^{-1} for 2a (Figure 6).

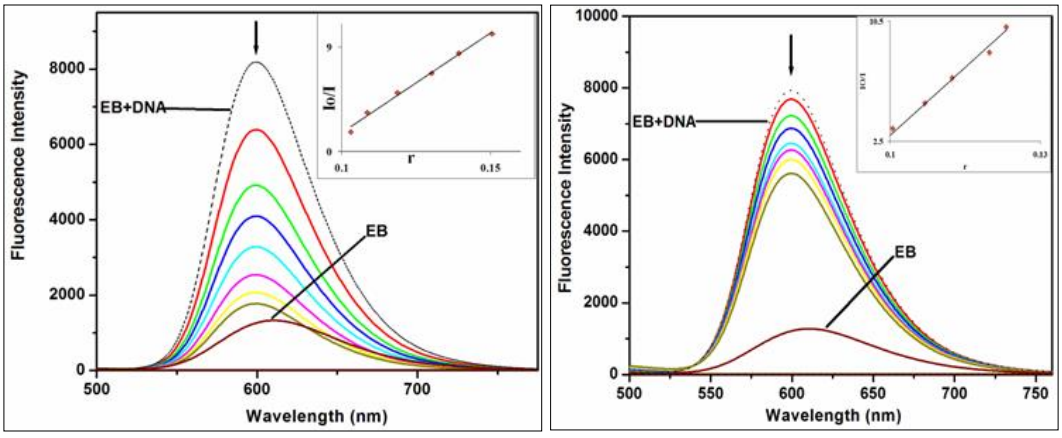

1a 2a

Fig 7: shows the fluorescence emission spectra of the CT-DNA-EB system at 25 °C with and without an increase in the concentration of the complexes 1a, and 2a in Tris HCl buffer (pH 7.2). When the concentration of the complexes grew, the emission intensity decreased, as seen by the arrow (↓). Io/I vs r inset

6. DNA cleavage activity

The interaction of pBR322 DNA with the newly synthesized Schiff base ligands HL_1 and HL_2, along with their metal complexes 1a and 2a, was studied using gel electrophoresis under oxidative (with hydrogen peroxide) and photolytic (with UV light) conditions. DNA cleavage ability was assessed by tracking the transformation of supercoiled circular DNA (Form I) into nicked (Form II) and linear (Form III) forms. Figures7.a and 7.b show the different DNA cleavage patterns observed during oxidative and photolytic treatments with HL_1, HL^2, and their metal complexes 1a and 2a. In the oxidative method (Figure 7a), the DNA control, DNA with H_2O_2, and ligands HL_1 and HL_2 (lanes 1–4) did not cause any noticeable DNA cleavage. In contrast, lanes 5 and 6, containing complexes 1a and 2a, showed effective conversion of supercoiled DNA (Form I) into the nicked form (Form II). Similarly, in the photolytic method (Figure 7b), the DNA control and both ligands (lanes 1–3) showed no cleavage. However, the presence of metal complexes in lanes 4 (1a) and 5 (2a) resulted in clear DNA strand scission, converting Form I into Form II [29].

These findings indicate that the metal complexes exhibit stronger DNA cleavage activity than the free ligands. This enhanced activity could be due to electron transfer from the donor atoms in the ligands to the positively charged metal ion, which may increase the lipophilicity of the complexes and improve their interaction with DNA [30].

Fig 8.(a). The metal complexes oxidatively cleaved supercoiled pBR322 DNA (0.2 µg, 33.3 µM) at 37 °C in a buffer of 5 mM Tris HCl/5 mM NaCl. 1st lane, DNA control: 2nd lane, DNA + H_2O_2 (1 mM); 3rd lane, DNA + H_2O_2 (1 mM) + HL_1; 4th lane, contains DNA + H_2O_2+HL_2; 5th lane contains DNA + H_2O_2 (1 mM) + 1a; 6th lane, contains DNA + H_2O_2 (1 mM) + 2a.

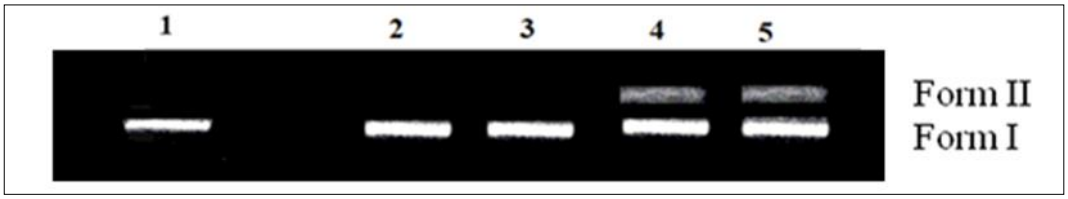

Fig 8.(b). Photoactivated cleavage of supercoiled pBR322 DNA by the complexes UV-light at 37 °C in 5 mM Tris HCl/5 mM NaCl buffer (long UV-365 nm). 1st lane, DNA control; 2nd lane, DNA + HL_1; 3rd lane, DNA + HL_2; 4th lane, DNA + 1a; 5th lane, DNA + 2a.

7. Biological studies

Antimicrobial activity

The antimicrobial activity of the synthesized Schiff base ligands HL_1 and HL_2 and their corresponding metal complexes (1a and 2a) was evaluated against selected bacterial and fungal strains using the agar well diffusion method. The results, summarized in Table 3 and Figure 8, revealed that the metal complexes exhibited significantly enhanced antimicrobial activity compared to their respective free ligands.

Among the tested compounds, complex 2a displayed the highest antimicrobial potency, showing pronounced inhibitory effects against both Gram-positive and Gram-negative bacterial strains. Furthermore, complex 2a demonstrated notable antifungal activity against Aspergillus niger and Candida albicans. The enhanced biological activity of the metal complexes may be attributed to chelation, which increases lipophilicity and facilitates the penetration of the complexes through microbial cell membranes. Although the synthesized complexes exhibited considerable antimicrobial efficacy, their activity remained lower than that of the standard reference drug.

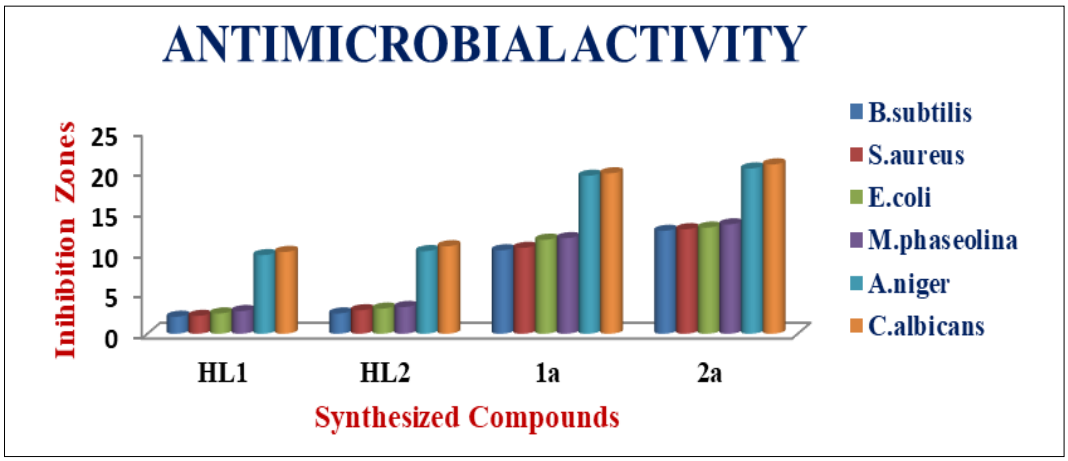

Fig 9: Graphical representation of the antimicrobial activity of Schiff bases (HL_1 & HL_2) and their metal complexes

Table 3: Schiff base and metal complex antimicrobial activity as inhibition zone diameters (mm) at 100 µg/ml concentration.

Compound	Anti Bacterial Activity				Antifungal Activity	
	Gram Positive Bacterium		Gram Negative Bacterium		A.niger	C.albicans
	B.subtilis	S.aureus	E.coli	K.pneomoniea		
HL_1	2.1	2.2	2.5	2.8	9.7	10.1
HL_2	2.5	2.9	3.1	3.3	10.2	10.8
1a	10.3	10.6	11.6	11.8	19.5	19.8
2a	12.7	12.9	13.1	13.5	20.4	20.9
Gentamycin Sulphate	29.1	31.6	30	29.3		
Nystatin					29.8	26.1

Anticancer activity (MTT assay)

The anticancer activity of the Schiff base ligands HL_1 and HL_2, along with their metal complexes 1a and 2a, was assessed using the MTT assay against MCF-7 (human breast cancer) and A-549 (human lung adenocarcinoma) cell lines. Doxorubicin, a well-established anticancer drug, served as the reference standard. The IC_{50} values of all synthesized compounds are presented in Table 4 and Figure 9. The cytotoxicity data indicated that all tested complexes exhibited significant cytotoxic effects against the MCF-7 cell line, surpassing their activity against the A-549 cell line. Among them, complex 2a exhibited the most pronounced cytotoxicity. Moreover, all metal complexes demonstrated enhanced activity compared to their corresponding free ligands, suggesting that metal coordination improved the anticancer potential of the compounds. The order of cytotoxicity was found to be $HL_1 < HL_2 < 1a < 2a$.

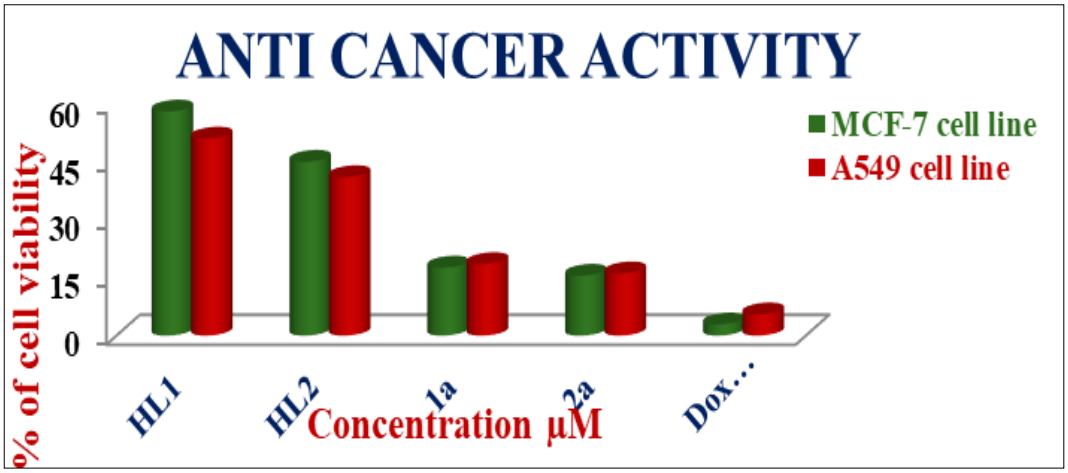

Fig 10: anticancer activity of Schiff bases and their metal complexes (1a & 2a) against MCF-7 and A549 cell lines

Table 4: Anticancer activity of schiff base and its metal complexes against MCF-7 (human breast cancer cell line) and A-549 (human lung adenocarcinoma cell line)

Compound	IC_{50}(MCF-7)	IC_{50}(A549)
HL_1	58	51
HL_2	45	41
1a	17.6	18.5
2a	15.5	16.1
Doxorubicin	2.9	5.5

Swiss-ADME analysis

The in silico design of a Schiff bases (HL1 & HL2) and their zink (II) metal complexes (1a & 2a) provided valuable insights into their theoretical biological activities. For a chemical compound to exhibit therapeutic potential, it must reach the target site within the body at adequate concentrations while retaining bioactivity for a duration sufficient to achieve the desired effects. ADME (Absorption, Distribution, Metabolism, and Excretion) analysis, increasingly utilized in early drug development, highlights these critical attributes. The findings from the ADME analysis are summarized in table 5. The Schiff base ligand (HL) demonstrated favorable alignment with all drug-likeness criteria, suggesting good pharmacokinetic potential. In contrast, the metal complexes (1a and 2a) failed to comply with two of Lipinski's rules, specifically due to their higher molecular weight and elevated Log P values.

These deviations indicate that the metal complexes may lack oral bioavailability, likely attributed to their flexible and polar nature. Isoenzymes, which play a pivotal role in pharmacokinetics and drug-drug interactions, were also evaluated [26]. The Schiff base and its complexes exhibit the potential to act as substrates or inhibitors of these isoenzymes, thereby influencing their enzymatic activity. Despite these limitations, both the Schiff bases and their metal complexes (1a and 2a) displayed promising pharmacokinetic responses, offering significant scope for further investigation in the context of drug development (Figure 10).

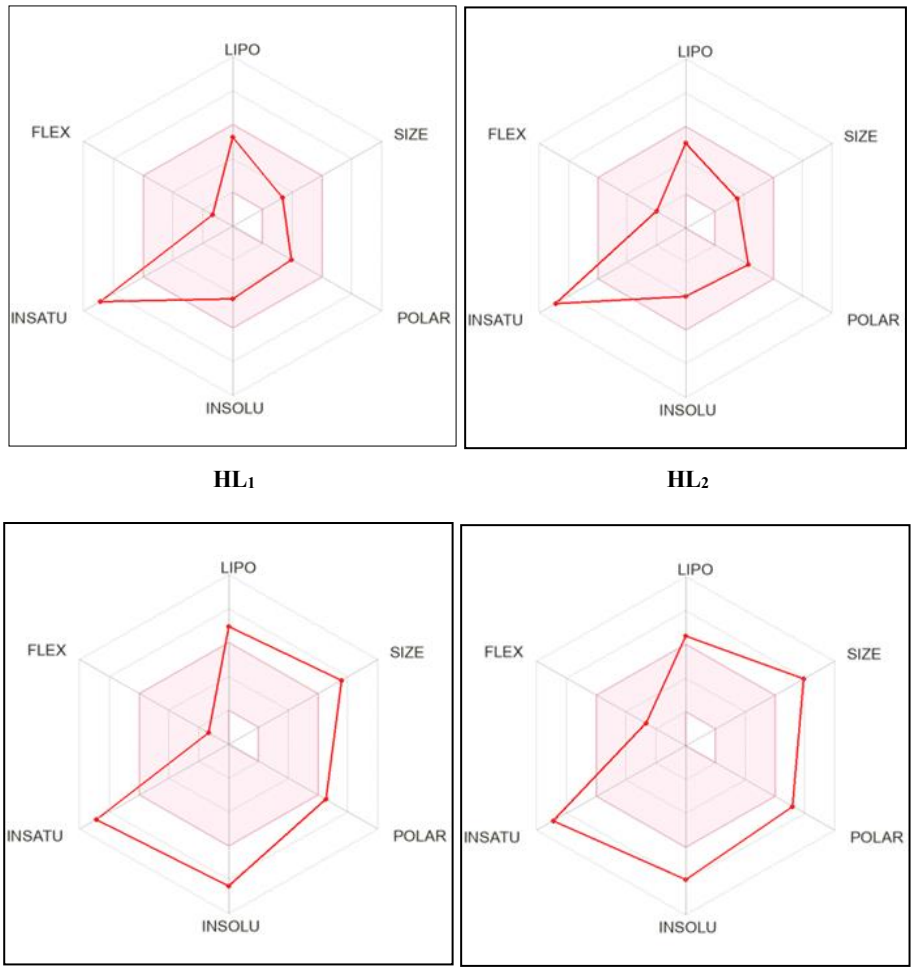

HL_1 **HL_2**

1a **2a**

Fig 10: Bioavailability radar for ligand (HL_1 & HL_2) and synthesized complexes (1a and 2a) within the domain borders of ADME properties, calculated by Swiss ADME. The colored zone of the radar is the suitable physicochemical space for oral

Table 5: The Swiss ADME tool evaluated various factors, such as physicochemical properties, lipophilicity, pharmacokinetics, drug-likeness, and medicinal chemistry for Schiff base ligand (HL1 & HL2) and their zink metal complexes (1a and 2a). The assessment results were presented in one-panel-per-molecule outputs

Compound	HL_1	HL_2	1a	2a
Physicochemical properties				
Molecular formula	$C_{15}H_{12}N_2OS$	$C_{15}H_{12}N_2O_2S$	$C_{30}H_{26}N_4O_4S_2Zn$	$C_{30}H_{26}N_4O_4S_2Zn$
Molecular weight (g/mol)	268.33 /mol	284.33 g/mol	636.06 g/mol	636.06 g/mol
Num. heavy atoms	19	20	41	41
Num. atom. heavy atoms	15	15	30	30
TPSA (Å2)	73.72 Å²	82.95 Å²	80.10 Ao	143.90 Å²
No. of H bond acceptor	3	4	6	6
No. of H bond donor	1	1	2	2
No. of rotatable bonds	2	3	2	2
Fraction Csp3	0.07	0.07	0.07	0.07
Molar refractivity	80.3	81.83	170.57	170.57
Lipophilicity				
Log Po/w (iLOGP)	2.68	2.63	0	0
Log Po/w (XLOGP3)	3.39	3.29	6.64	6.64
Log Po/w (WLOGP)	4.06	3.76	7.5	7.5
Log Po/w (MLOGP)	2.24	1.65	1.86	1.86
Log Po/w (SILICOS-IT)	5	4.52	2.28	2.28
Consensus Log Po/w	3.53	3.17	3.66	3.66
Water Solubility				
Log S (ESOL)	-4.28	-4.03	-8.38	-8.38
Solubility (mg/ml; mol/l)	1.41e-02 mg/ml ; 5.24e-05 mol/l	2.64e-02 mg/ml ; 9.28e-05 mol/l	2.67e-06 mg/ml ; 4.20e-09 mol/l	2.67e-06 mg/ml ; 4.20e-09 mol/l
Class (soluble)	Moderately soluble	Moderately soluble	Poorly soluble	Poorly soluble
Log S (Ali)	-4.93	-4.71	-9.46	-9.46
Solubility (mg/ml; mol/l)	3.16e-03 mg/ml ; 1.18e-	5.58e-03 mg/ml ; 1.96e-05	2.19e-07 mg/ml ; 3.44e-10	2.19e-07 mg/ml ; 3.44e-10

	05 mol/l	mol/l	mol/l	mol/l
Class(soluble)	Moderately soluble	Moderately soluble	Poorly soluble	Poorly soluble
Pharmacokinetics				
GI absorption	High	High	Low	Low
BBB penetration	Yes	No	No	No
Log Kp (cm/s)	-5.32 cm/s	-5.70 cm/s	-5.47 cm/s	-5.47 cm/s
Drug-likeness				
Lipinski	Yes; 0 violation	Yes; 0 violation	Yes; 1 violation: MW>500	Yes; 1 violation: MW>500
Bioavailability Score	0.55	0.55	0.55	0.55
Medicinal Chemistry				
Drug-likeness	No	yes	No	No
Synthetic accessibility	2.64	2.68	5.45	5.45

Three novel Schiff base metal complexes 1a and 2a have been synthesized from a Schiff base ligands HL_1 and HL_2, which is characterized by elemental analysis and spectral analysis such as FT-IR, UV-Vis, Mass, and TGA, which revealed that the Zn(II) complexes exhibited an octahedral geometry, coordination water molecule is present in the Zn(II) complexes which were confirmed by FT-IR and TGA. DNA interaction studies revealed that two synthesized complexes bind via intercalative mode. DNA interaction studies concluded that the synthesized three complexes cleaved into nicked or linear form in both cleavage modes. Biological studies performed by antimicrobial, and cytotoxicity have shown that the 2a complex have shown enhanced activity compared to a complex and their respective ligands.

Acknowledgements
We would like to express our sincere thanks to the Head, Department of Chemistry for providing the necessary facilities for carrying out the work successfully. We are thankful to Director, CFRD, Osmania University and the Director, NITW for providing spectral and analytical data.

References

1. McQuitty RJ. Metal-based drugs. Sci. Prog,2014:97(1):1-19.
2. Sodhi RK. Metal Complexes in Medicine: An Overview and Update from Drug Design Perspective. Cancer Ther. Oncol. Int, J., 2019, 14(1).
3. Ramesh G, Daravath S, Swathi M, Sumalatha V, Shankar DS, Shivaraj. Investigation on Co(II), Ni(II), Cu(II) and Zn(II) complexes derived from quadridentate salen-type Schiff base: Structural characterization, DNA interactions, antioxidant proficiency and biological evaluation. Chemical Data Collections,2020:28:100434.
4. Liu X, Hamon JR. Recent developments in penta-, hexa- and heptadentate Schiff base ligands and their metal complexes. Coord. Chem. Rev,2019:389:94-118.
5. Sarker D, Karim MR, Haque MM, Zamir R, Asraf MA. Copper (II) Complex of Salicylaldehyde Semicarbazone: Synthesis, Characterization and Antibacterial Activity. Asian Journal of Chemical Sciences,2019:6(4):1-8.
6. Sarker D, Reza MY, Haque MM, Zamir R, Asraf MA. Synthesis, Characterization, Antibacterial and Thermal Studies of Cu (II) Complex of Thiophene-2-aldehyde Semicarbazone. Asian Journal of Applied Chemistry Research,2019:(4):1-10.
7. Ndagi U, Mhlongo N, Soliman ME. Metal complexes in cancer therapy - an update from drug design perspective. Drug design, development and therapy,2017:11:599-616.
8. Shahabadi N, Mohammadi S. Synthesis Characterization and DNA Interaction Studies of a New Zn(II) Complex Containing Different Dinitrogen Aromatic Ligands. Bioinorganic Chemistry and Applications, 2012, 1-8.
9. Bastaki SA. Diabetes mellitus and its treatment. Inter J Diabetes Metabolism, 13(3):111.
10. Whitcomb DC, Lowe ME. Human Pancreatic Digestive Enzymes. Dig Dis Sci,2005:52:1-17.
11. Omer MAS, Liu J, Deng W, Jin N. Syntheses, crystal structures and antioxidant properties of four complexes derived from a new Schiff base ligand (N1E,N2E)-N1,N2-bis(1-(pyrazin-2-yl)ethylidene)ethane-1,2 diamine. Polyhedron,2014:69:10-4.
12. EI-ajaily MM, Maihub AA, Mahanta UK, Badhei G, Mohapatra RK, Das PK. MIXED LIGAND COMPLEXES CONTAINING SCHIFF BASES AND THEIR BIOLOGICAL ACTIVITIES: A SHORT REVIEW. Rasayan J. Chem,2018:11(1):166-174.
13. Pahonțu E, Ilies DC, Shova S, Paraschivescu C, Badea M, Gulea A, *et al*. Molecules,2015:20(4):5771-5792.
14. Daravath S, Rambabu A, Shankar DS, Shivaraj. Structure elucidation of copper(II), cobalt(II) and nickel(II) complexes of benzothiazole derivatives: Investigation of DNA binding, nuclease efficacy, free radical scavenging and biocidal properties. Chem Data Collections,2019:24:100293.
15. Daravath S, Vamsikrishna N, Ganji N, Venkateswarlu K, Shivaraj. Synthesis, characterization, DNA binding ability, nuclease efficacy and biological evaluation studies of Co(II), Ni(II) and Cu(II) complexes with benzothiazole Schiff base. Chem Data Coll,2018:17(18):159-168.
16. Pichandi M, Shanmugam S. Synthesis, characterization of Schiff base metal complexes with 1, 3 propanediamine as secondary chelates and their DNA binding, DNA cleavage, cytotoxicity, antioxidant and activities Author links open overlay panel. J. Mol.Structure,2024:1307:137932.
17. Matin MM, Uzzaman M, Chowdhury SA, Bhuiyan MMH. *In vitro* antimicrobial, physicochemical, pharmacokinetics and molecular docking studies of benzoyl uridine esters against SARS-CoV-2 main protease. J biomo Dyn,2020:40(8):3668-3680.
18. Babu KJ. Synthesis, Spectroscopic Characterization, DNA Binding, and Biological Evaluation of Zn(II) Complexes Derived from 5-Cyclohexylanisidine-Based Schiff Bases. INT J INNO RES MULT FIELD,2025:11(62):194-205.

19. Gopichand K, Mahipal V, Rao NN, Ganai AM, Rao PV. Co(II), Ni(II), Cu(II), and Zn(II) complexes with Benzothiazole Schiff base ligand: Preparation, Spectral Characterization, DNA Binding, and *In vitro* Cytotoxic Activities. Res in Chem,2023:5:100868.
20. Nakamoto K. Infrared and Raman Spectra of Inorganic and Coordination Compounds. Wiley-Interscience, 1997, 5.
21. Devi J, Yadav M, Kumar A, Kumar A. Synthesis characterization biological activity and QSAR studies of transition metal complexes derived from piperonylamine Schiff bases. Chemical papers,2018:72:2479-2502.
22. Ramesh G, Daravath S, Babu KJ, Dharavath R, Ranjan A, Ayodhy D, *et al*. Design, Synthesis, Structural Investigation and Photo Induced Biological Investigations of Co(II), Ni(II) and Cu(II) Complexes Derived from N,O Donor Schiff Bases. J. Fluer,2024:34:2087-2108.
23. Babu KJ. Zn(II) Complexes of 6-Aminobenzothiazole-Based Schiff Bases: Synthesis, Spectroscopic Characterization, DNA Binding Studies and Biological Investigations. International J Eng Res & Tech, 2026, 15(04).
24. Jyothi N, Daravath S, Swathi M, Jagadeshbabu K, Ganji N, Shivaraj. Synthesis, geometry optimization and non-isothermal kinetic parameters of copper(II), nickel(II) and cobalt(II) complexes of 5-(trifluoromethyl)-2-methoxybenzenamine: DNA binding, cytotoxicity, antioxidant and antimicrobial activity. J Mol Stru,2024:129(1):136529.
25. Babu KJ. Synthesis and Biological Profiling of Zn(II) Complexes with 6-Aminobenzothiazole-Derived Schiff Bases: Insights into DNA Binding and Spectroscopic Properties. J Emer Tech Inn Research,2026:13(4):j300-j315.
26. Babu KJ, Ayodhyaa D, Shivaraj. Comprehensive investigation of Co(II), Ni(II) and Cu(II) complexes derived from a novel Schiff base: Synthesis, characterization, DNA interactions, ADME profiling, molecular docking, and *in-vitro* biological evaluation. Results in Chemistry,2023:6:101110.
27. Anamika H, Sanaul IM, Mukti M, Samim K. Synthesis, structural characterization of dinuclear copper(II) complexes based on Schiff base derived ligands and their impacts on DNA-binding affinities. Inorg. Chi Acta,2023:557:121720.
28. Swathi M, Ayodhya D, Shivaraj. Synthesis, Characterization, Investigation of DNA Interactions and Biological Evaluation of Co(II), Ni(II), Cu(II) and Zn(II) Complexes with Newly Synthesized 2-methoxy 5-trifluoromethyl benzenamine Schiff Base. Journal of Fluorescence,2025:35:5301-5317.
29. Babu KJ, Daravath S, Swathi M, Ayodhya D, Shivaraj. Synthesis, anticancer, antibacterial, antifungal, DNA interactions, ADMET, molecular docking, and antioxidant evaluation of novel Schiff base and their Co(II), Ni(II) and Cu(II) complexes. Res Chem,2023:6:101121.
30. Swathi, Ayodhya D, Shivaraj. Design, structural characterization, DNA interaction studies, antibacterial, antioxidant, and cytotoxicity studies of Co(II), Ni(II), Cu((II), Zn((II) complexes containing 2-methoxy 5-trifluoromethyl benzenamine Schiff base. Results in Chemistry,2024:7:101231.